Effects of Head Shape on EEG's and MEG's

B. NEIL CUFFIN

Abstract—**This paper presents results of computer modeling studies of the effects of head shape on electroencephalograms (EEG's) and magnetoencephalograms (MEG's) and on the localization of electrical sources in the brain using these measurements. The effects of general, nonspherical head shape on EEG's and MEG's are determined by comparisons of EEG and MEG maps from nonspherical head models with corresponding maps from a spherical head model. The effects on source localization accuracy are determined by calculating moving dipole inverse solutions in a spherical head model using EEG's and MEG's from the nonspherical models and comparing the solutions with the known sources.**

It was found that nonspherical head shape can produce significant changes in the maps produced by some sources in the cortical region of the brain. However, it was also found that such deviations of the head from sphericity produce localization errors of less than approximately 1 cm. No significant differences in the effects of such deviations on EEG's and MEG's were found. Finally, it was found that most such deviations do not cause a dipolar source which is perpendicular to the surface of the head model to produce a significant magnetic field; such a source produces zero magnetic field in a sphere.

Introduction

INFORMATION about the effects of the volume conductor properties of the head on electroencephalograms (EEG's) and magnetoencephalograms (MEG's) is necessary for accurate localization of electrical sources in the brain. For example, information showing that the low conductivity of the skull "smears" the EEG produced by a source in the brain [1] and makes it appear deeper in the brain than it actually is has been used to develop localization methods which deal with this effect. Likewise, information about the effects of other volume conductor properties of the head, such as its shape or local variations in skull conductivity, on EEG's and MEG's is necessary. This paper presents results concerning the effects of head shape on EEG's and MEG's and source localization.

Only a limited number of studies of the effects of head shape on EEG's have been performed. In a computer modeling study, Witwer *et al.* [2] found that the position of the external surface of a model of a cat head can have significant effects on the EEG produced by a source in the brain. Henderson *et al.* [3] found localization errors of up to 1.9 cm for sources in a saline-filled skull. Localization errors of up to 3.0 cm were obtained by Smith *et al.* [4] for implanted sources in a human head. Finally, He *et al.* [5] found localization errors of 1.0 cm or less for implanted sources in a cat brain. In these last three studies, it is not known if head shape alone is the cause of the localization errors since noise and other experimental errors are also present.

Two experimental studies [6], [7] of the effects of head shape on MEG's have found significant distortion of the maps produced by sources in skulls filled with conductive paste or gel and localization errors of up to 1.0 cm. The results of these studies are somewhat inconclusive since there was no scalp on the skulls. A computer modeling study [8] has found that omitting the skull and scalp in a realistic model of the head can produce localization errors of up to 1.5 cm. Similar errors were obtained in a more recent computer modeling study [9] comparing a realistic head model and simple spherical ones. The results of these computer modeling studies are also somewhat inconclusive since only one realistic head model was investigated in each study.

In summary, only rather limited data are available concerning the effects of head shape on EEG's and MEG's and source localization. In this paper, results of detailed computer modeling studies of general, large-scale deviations of the head from sphericity are presented. The effects are evaluated by comparing results from various nonspherical head models with those from a spherical model. The effects on both EEG and MEG maps and on inverse solutions using these data are evaluated.

Methods

The basic computer model of the head used in these investigations is shown in Fig. 1. This model contains three regions with different electrical conductivities which represent the brain, skull, and scalp. The conductivity of the skull region is 1/80th of that of the brain and scalp regions. All of the surfaces of the model are composed of plane triangular elements so that previously developed methods of calculating the electric potentials (EEG's) [10] and magnetic fields (MEG's) [11] for electrical sources in the brain region can be used. The calculated potentials are the numerical solution of the surface integral equation for the potentials produced by current dipole sources (P_x, P_y, and P_z) in the model. These calculated potentials are the average potential on a triangular element. To improve the accuracy of the calculations, a greater density of triangles is used on the portions of the surfaces near the sources. Also, a recently developed method [12] is used to further improve the accuracy of the potential calculations. This method greatly reduces the inaccuracies in the calcula-

Manuscript received September 6, 1988; revised April 25, 1989. This work was supported by National Institutes of Health Grant NS22703.

The author is with the Francis Bitter National Magnet Laboratory, Massachusetts Institute of Technology, Cambridge, MA 02139.

IEEE Log Number 8931537.

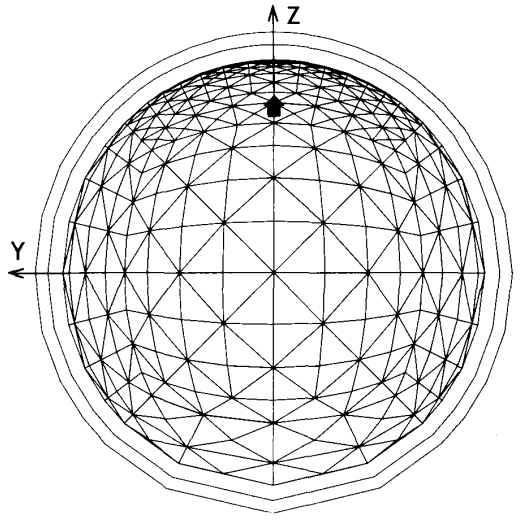

Fig. 1. Side view of the basic head model showing the triangular elements on the brain-skull surface; the outlines of the other two surfaces are also shown. Each surface is composed of 1088 triangles for a total of 3264 in the model. The radii of the surfaces are 8.4, 9.0, and 9.5 cm; the conductivities of the brain and scalp regions are $3.3 \times 10^{-3}\ \Omega/\text{cm}$ and the conductivity of the skull is $4.1 \times 10^{-5}\ \Omega/\text{cm}$. A P_z dipole is shown on the Z axis at a depth of 3.1 cm below the surface of the scalp which is 2.0 cm below the surface of the brain.

tions caused by the large differences between the conductivity of the skull region and the rest of the model. As seen later, this basic model can be modified to represent any desired head shape. In this study, it is modified to represent a number of basic, nonspherical head shapes and to represent measurements over various areas of the head surface.

The accuracy of these potential and field calculations is shown by comparing the results in Fig. 2, for which the model has a spherical shape, with the exact values obtained from mathematical equations for such a multilayer sphere. The EEG's for this spherical (S) model agree to within 2 percent with the values from the equations while the MEG's show even better agreement. For this and all other models, the EEG's are the potentials on the triangles with reference to a triangle on the bottom of the model and the MEG's are the component of magnetic field perpendicular to and 1.0 cm above the center of a triangle. There are some small asymmetries in the EEG maps because of the asymmetrical location of the triangle used for the reference point and because the triangles used in the measurement grid are not exactly symmetrically located. Note that all the values in the MEG map for the P_x dipole are zero. This is because a dipolar source which is perpendicular to the surface of a sphere produces zero magnetic field. This is a special property of magnetic fields for such a dipole in a sphere and it is important to know if deviations of the head from sphericity cause such sources to produce significant fields.

Source localization is done using the moving dipole inverse solution method. In this method, a dipolar source is

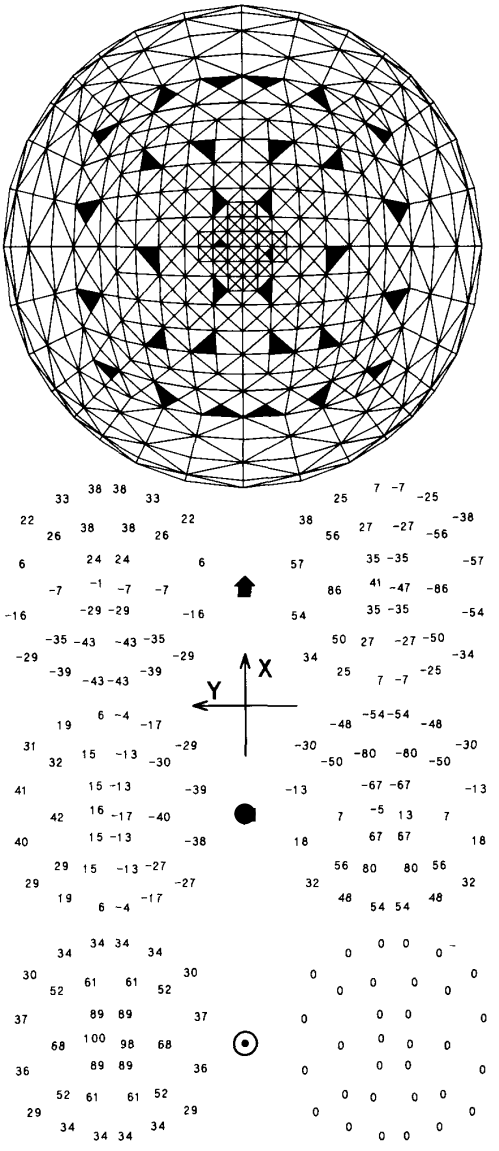

Fig. 2. Top view of the spherical (S) model showing the 32 (darkened) triangles used as points in a measurement grid. Maps of the EEG's (left) and MEG's (right) at these triangles are shown below for the three indicated dipole orientations. The coordinate axes shown apply to both the model and the maps. The EGG's are in microvolts $\times 10^{-1}$ and the MEG's in picotesla $\times 10^{-2}$ for 5 μA·cm dipoles 3.1 cm below the surface of the model.

moved about in a model of the head while its amplitude and orientation are also varied to obtain the least-squares fit between measured EEG's or MEG's and those produced by the dipole. As the method is used here, the "measured" data are actually EEG's or MEG's from the computer model of the head. The solutions are calculated in a multilayer sphere with the same radii and conductivities as the model in Fig. 1; the solutions are calculated for the EEG's or MEG's from the 32 grid points on each model. This grid is large enough and has enough points

TABLE I
INVERSE SOLUTIONS FOR P_x SOURCES. MODEL TYPE IS AS DESCRIBED IN THE TEXT AND FIGS. *D* INDICATES A EEG OR MEG DATA SOLUTION, *F* IS THE FIT AS DEFINED IN (1), IN PERCENT, BETWEEN THE MODEL DATA AND THE SOLUTION DIPOLE DATA, DEPTH, X, AND Y ARE THE SOLUTION LOCATION IN CM, P_x, P_y, AND P_z ARE THE *NORMALIZED* SOLUTION DIPOLE COMPONENTS, AND DIS IS THE DISTANCE IN CM OF THE SOLUTION DIPOLE FROM THE ACTUAL DIPOLE. THE "I" MODEL LINE GIVES THE IDEAL SOLUTION

MODEL	D	F	DEPTH	X	Y	P_x	P_y	P_z	DIS
I		0	3.10	0.00	0.00	1.00	0.00	0.00	
S	E	3	3.17	0.22	−0.03	1.00	0.00	0.02	0.23
	M	0	3.10	0.00	0.00	0.99	0.00	0.00	0.00
NE	E	7	4.05	−0.01	−0.01	1.52	0.00	−0.09	0.95
	M	20	3.81	−0.30	0.00	1.23	0.00	0.07	0.77
NEB	E	8	4.41	−1.08	−0.16	1.36	−0.01	−0.39	1.71
	M	8	4.33	−0.06	0.00	1.62	0.00	0.02	1.23
WE	E	5	3.63	−0.05	−0.01	1.14	0.00	−0.07	0.53
	M	8	3.08	−0.32	0.00	0.96	0.00	0.05	0.32
WEB	E	6	4.05	−0.53	0.04	1.16	0.00	−0.25	1.09
	M	7	3.41	−0.03	0.00	1.15	0.00	0.01	0.31
WES	E	6	3.57	0.07	0.30	1.24	0.00	−0.03	0.56
	M	16	3.53	−0.32	0.05	1.12	−0.01	0.06	0.54
BP	E	4	3.26	0.18	−0.30	1.16	0.00	0.02	0.38
	M	27	3.49	0.00	0.52	1.06	0.00	0.00	0.65

TABLE II
INVERSE SOLUTIONS FOR P_y SOURCES

MODEL	D	F	DEPTH	X	Y	P_x	P_y	P_z	DIS
I		0	3.10	0.00	0.00	0.00	1.00	0.00	
S	E	1	3.14	0.00	−0.05	0.00	0.97	−0.01	0.06
	M	1	3.09	−0.01	0.00	0.00	1.00	0.00	0.01
NE	E	11	3.64	−0.33	−0.12	0.00	0.93	−0.01	0.64
	M	17	2.90	−0.17	−0.01	0.00	0.88	0.00	0.26
NEB	E	6	4.05	−0.46	−0.30	0.00	1.20	−0.06	1.10
	M	8	3.84	−0.05	0.00	0.00	1.37	0.00	0.74
WE	E	5	3.38	−0.34	−0.08	0.00	0.97	−0.01	0.45
	M	9	2.79	−0.19	−0.01	0.00	0.87	0.00	0.36
WEB	E	4	3.68	−0.22	−0.15	0.00	1.21	−0.04	0.64
	M	9	3.69	−0.06	0.00	0.00	1.29	0.00	0.59
WES	E	8	3.58	−0.50	0.26	0.00	1.00	0.12	0.74
	M	13	2.91	−0.19	0.01	0.00	0.89	0.00	0.27
BP	E	9	3.06	−0.11	−0.26	0.00	0.75	0.20	0.29
	M	8	2.57	−0.02	−0.73	0.00	0.56	0.06	0.90

on it so that the inverse solutions are not sensitive to small changes in its size or in the number and distribution of points on the grid [13]. As part of these calculations, a measure of the closeness of the fit (F) between the EEG's or MEG's of the computer model and those of the moving dipole solution is calculated. This measure is defined as

$$F = \frac{\sqrt{\sum_{i=1}^{32} (C_i - M_i)^2}}{\sqrt{\sum_{i=1}^{32} (C_i)^2}} \qquad (1)$$

where C_i is the computer model data at the ith grid point and M_i is the moving dipole solution data. The value of F should be zero if the computer model is also a sphere. For the EEG solutions, the effects of the different conductivity layers are taken into account using the method described in the Appendix. Such layers have no effects on the MEG solutions [14].

Further indication of the accuracy of the potential and field calculations is provided by the inverse solutions for the *S* model given Tables I–III. The maximum localization error, i.e., the maximum "DIS" value in the tables, is 0.23 cm for the EEG solutions and 0.01 cm for the MEG solutions for the P_x and P_y dipoles. The MEG solution for the P_z dipole requires a different interpretation than the other solutions. Ideally, the amplitude of the solution should be zero. Therefore, if the amplitude of the solution is zero or small as compared to the actual P_z source, then its location is not important. In addition, if the solution amplitude is small and has a large F value, this can be taken as an indication that there really is not a detectable dipolar source present and that the solution is just a result of noise. On these bases, the MEG solution for the P_z dipole is quite good. Since the *S* model has the same dimensions and conductivities as the multilayer

TABLE III
INVERSE SOLUTIONS FOR P_z SOURCES

MODEL	D	F	DEPTH	X	Y	P_x	P_y	P_z	DIS
I		0	3.10	0.00	0.00	0.00	0.00	1.00	
S	E	1	3.10	0.06	−0.01	−0.01	0.00	1.00	0.06
	M	91	−0.98	−5.79	0.78	0.00	0.00	0.00	6.28
NE	E	6	3.60	0.17	−0.03	−0.14	0.04	1.10	0.53
	M	67	2.97	3.25	−0.01	0.06	0.00	−0.03	3.25
NEB	E	2	4.13	0.56	−0.06	−0.34	0.01	1.39	1.17
	M	31	4.49	2.73	0.00	0.10	0.00	−0.06	3.06
WE	E	3	3.32	0.06	−0.01	−0.10	0.00	0.98	0.23
	M	17	3.56	2.00	0.00	0.05	0.00	−0.02	2.05
WEB	E	2	3.62	0.26	0.01	−0.16	−0.01	1.14	0.59
	M	15	4.01	−2.93	0.00	0.08	0.00	0.05	3.07
WES	E	4	3.32	0.03	−0.09	−0.10	0.12	1.02	0.24
	M	61	3.90	1.45	−0.36	0.08	−0.05	−0.02	1.69
BP	E	2	3.38	0.06	−0.32	−0.01	0.21	1.16	0.43
	M	11	3.15	−0.02	1.79	0.00	−0.17	0.05	1.79

sphere used in the inverse solution calculations, these localization errors are produced by the numerical calculation methods; the small magnitude of these errors indicates that the methods are quite accurate.

RESULTS

Results for six nonspherical models are given in Figs. 3–8 and in Tables I–III. With the exception of the skull layer in the BP model, the scalp and skull layers in these models have the same thicknesses as in the *S* model, i.e., the scalp layer is 0.5 cm and the skull layer is 0.6 cm. For those models in which the surfaces and the sources are rotated to the back or side, the P_x, P_y, and P_z designations for the sources are retained even though the actual dipole orientations are changed to be parallel or perpendicular to the adjacent surface.

The values in the EEG maps in Fig. 3 for the P_x and P_z dipoles in the NE model are generally larger than those for the *S* model. There are also asymmetries in these maps with respect to the X axis; the (absolute) values over the negative X axis are significantly larger than those over the positive X axis. The EEG map for the P_y dipole is similar to that for the *S* model, except that the peak values are at the edge of the grid rather than inside it. The MEG maps for the P_x and P_y dipoles are similar to those for the *S* model, except for the same asymmetry with respect to the X axis as for the EEG maps. The values in the MEG map for the P_z dipole are small as compared to those for the P_x and P_y dipoles; the pattern in this map is not a simple dipolar one. The maximum localization errors for both the EEG and MEG solutions are less than 1 cm. The amplitude of the MEG solution for the P_z dipole is quite small and its *F* value is quite large which is consistent with the nondipolar pattern of the associated map. The *F* values for the MEG solution for the P_x dipole and for both the EEG and MEG solutions for the P_y dipole are significantly larger than for the *S* model. Additional solutions were calculated for a multilayer sphere having an external radius of 7.2 cm rather than 9.5 cm and the same scalp and skull thicknesses. The localization errors for these solutions are all less than the corresponding values in the tables except for the MEG P_y solution which increased from 0.26 to 1.06 cm; the *F* values of these solutions are the same as the corresponding ones in the tables.

The EEG maps for the NEB model in Fig. 4 show the same pattern of differences from the *S* model as do the maps for the NE model, but the differences are larger. However, the MEG P_x and P_y maps are nearly symmetrical and are rather similar to those for the *S* model. The values in the MEG P_z map are much smaller than for the NE model. The localization errors are approximately twice as large as those for the NE model. The EEG P_x and P_y solutions are shifted in the negative X direction and a significant P_z component appears in the P_x solution. An opposite but smaller shift occurs in the EEG P_z solution and a significant P_x component appears. The localization errors in the MEG solutions are primarily in depth; there is little or no shifting of the solutions. The amplitude of the MEG P_z solution is quite small and its *F* value is large. As for the NE model, solutions were also calculated for a multilayer sphere with an external radius of 7.2 cm. These solutions show the same pattern of localization errors, but the maximum error is less than 1 cm.

The differences in both the EEG and MEG maps of the WE model in Fig. 5 as compared to those of the *S* model are similar to the differences for the NE model, except that they are smaller. All localization errors are less than 1 cm and are generally smaller than for the NE model. The MEG P_z solution has a small amplitude, but its *F* value is significantly smaller than for the *S* model.

Likewise, the differences in both the EEG and MEG maps for the WEB model in Fig. 6 are similar to but smaller than those for the NEB model. The localization errors are also all smaller than for the NEB model and with the exception of the EEG P_x solution are less than 1 cm. The MEG P_z solution amplitude is quite small, but its *F* value is significantly smaller than for the *S* model.

All three EEG maps for the WES model in Fig. 7 have the typical asymmetry with respect to the X axis seen in previous EEG maps. In addition, there is a significant asymmetry with respect to the Y axis in the EEG P_y map. The MEG P_x and P_y maps are asymmetrical with respect to both the X and Y axes. The values in the MEG P_z map

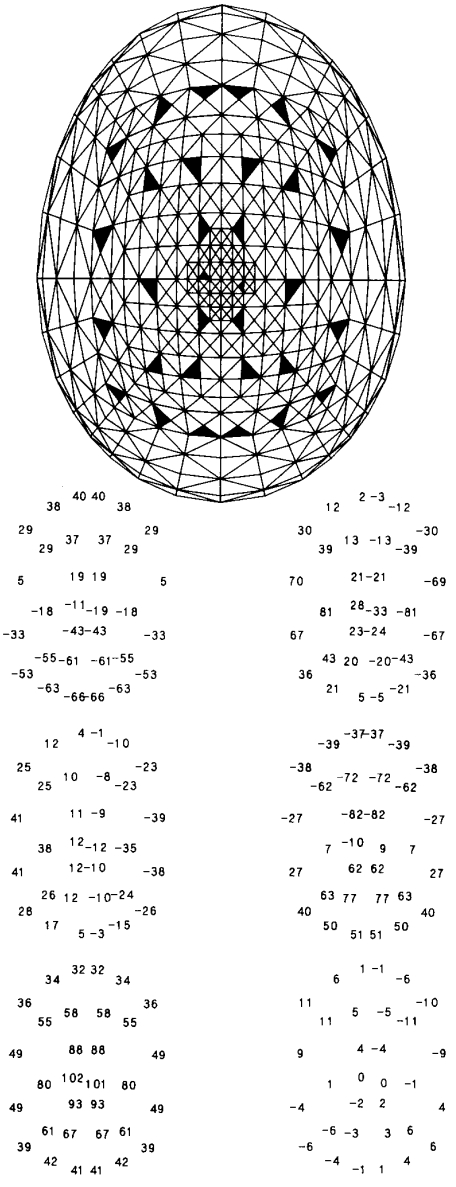

Fig. 3. The narrow ellipsoidal (NE) model. This model has the same overall length on the X axis as the S model in Fig. 2, but it has a circular cross-section in the Y-Z plane with an external radius of 7.2 cm.

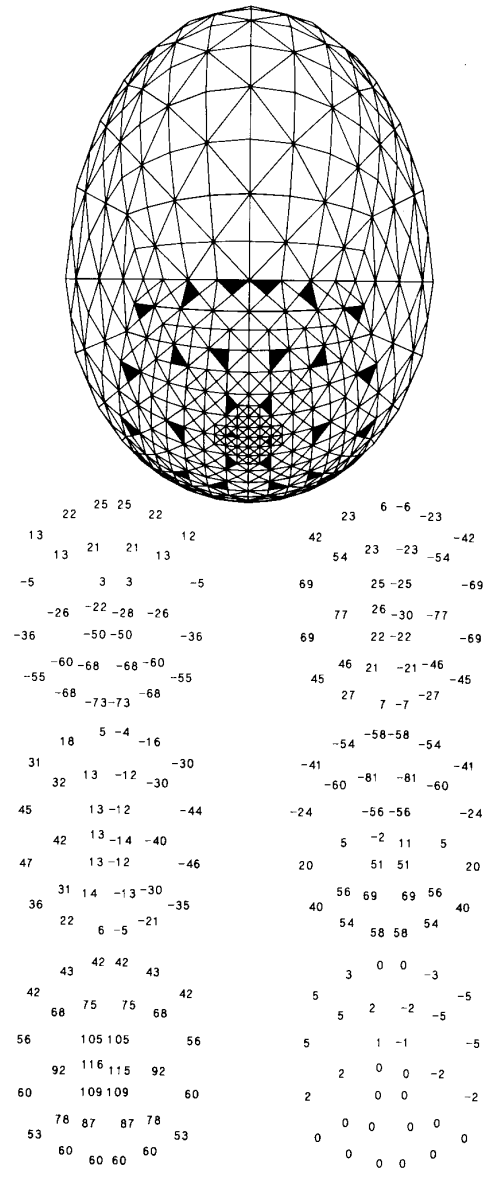

Fig. 4. The narrow ellipsoidal (NEB) model with the grid rotated towards the back of the model. The parameters of this model are the same as those of the NE model of Fig. 3 except that the grid and dipolar sources are rotated by 45° towards the negative X axis. For clarity, the maps present the grid as viewed from above the center of the grid.

are still relatively small. All localization errors are less than 1 cm. The F values for the MEG P_x and P_y solutions are significantly larger than for the S model. The MEG P_z solution has a small amplitude and a large F value.

The values in the EEG P_x and P_z maps for the BP model in Fig. 8 are generally larger than those for the S model. There is a shift in the zero-crossing line in the negative Y direction in the EEG P_y map. The MEG P_x map is asymmetrical with respect to the Y axis, while the entire MEG P_y map is shifted in the negative Y direction. The MEG P_z map has some significant values and looks like a map for a negative P_y dipole shifted in the positive Y direction. All localization errors are less than 1 cm. While the EEG P_y map is shifted significantly in the negative Y direction, the solution is shifted only slightly in that direction; however, a significant P_z component appears in the solution. The F value for the MEG P_x solution is significantly larger than for the S model. The MEG P_y solution is shifted 0.73 cm in the negative Y direction which is consistent with

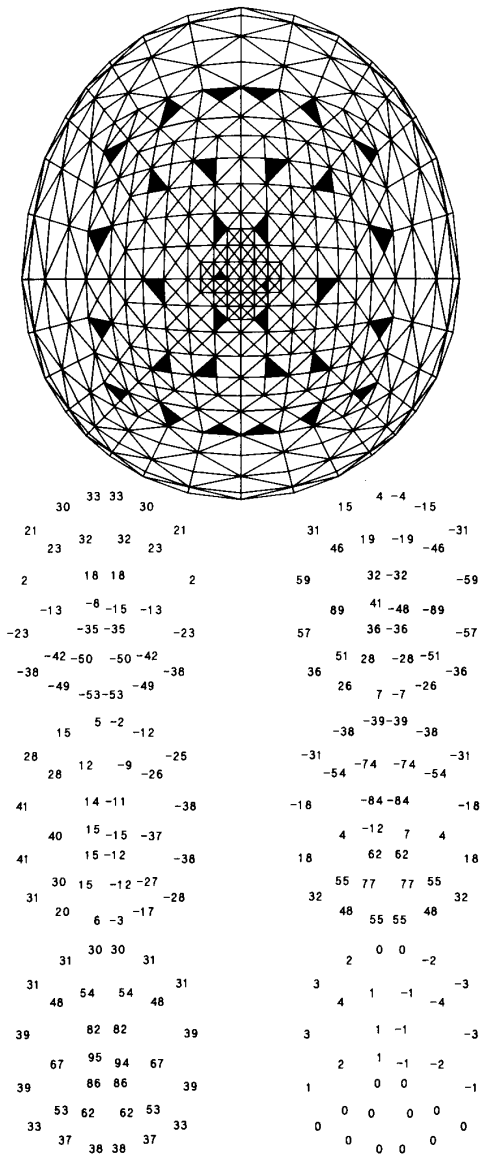

Fig. 5. The wide ellipsoidal (WE) model. This model has the same overall length on the X axis as the *S* model in Fig. 2, but it has an ellipsoidal cross section in the Y-Z plane with a major axis of 17.4 cm on the Y axis and a minor axis of 14.4 cm on the Z axis.

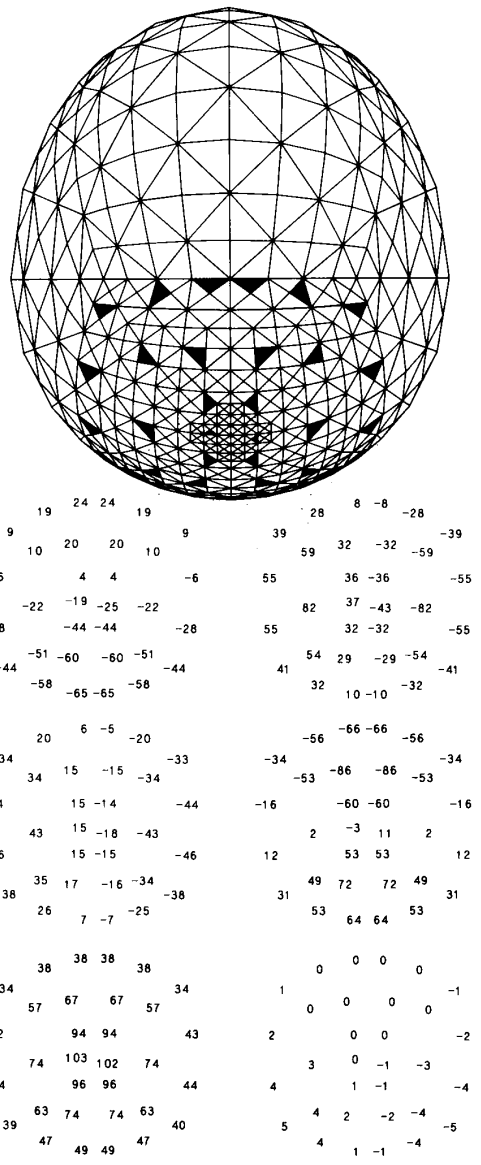

Fig. 6. The wide ellipsoidal (WEB) model with the grid and dipolar sources rotated by 45° towards the back of the model.

the shift in the map. Its amplitude is also significantly smaller than the actual source. The MEG P_z solution is located approximately on the "brain pan" surface. The relatively small F value for this solution indicates that the secondary source on the surface is well represented by a dipole. The amplitude of the solution is less than 20 percent of the actual dipole amplitude. In additional results not presented here, it was found that the effects of the brain pan surface decrease rapidly for sources more distant from that surface than are the sources in the BP model.

Discussion

These results indicate that the general, nonspherical shape of the head can have significant effects on the EEG and MEG maps for some cortical sources. However, these results also indicate that such deviations of the head from sphericity produce localization errors of approximately 1 cm or less when a sphere of appropriate size is used for the inverse solution calculations. Such a sphere need only have a radius which is approximately equal to the average radius of the region of the head on which the measure-

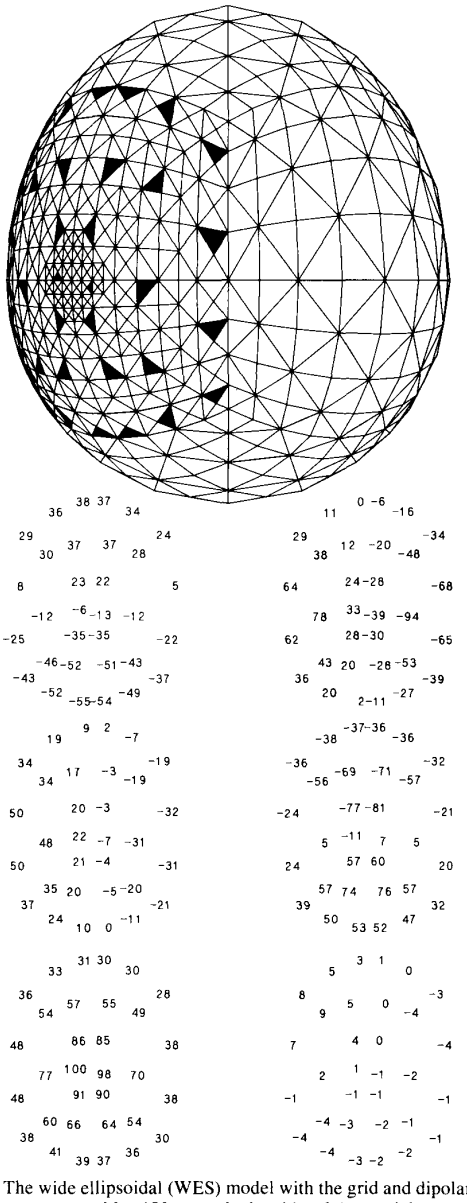

Fig. 7. The wide ellipsoidal (WES) model with the grid and dipolar sources rotated by 45° towards the side of the model.

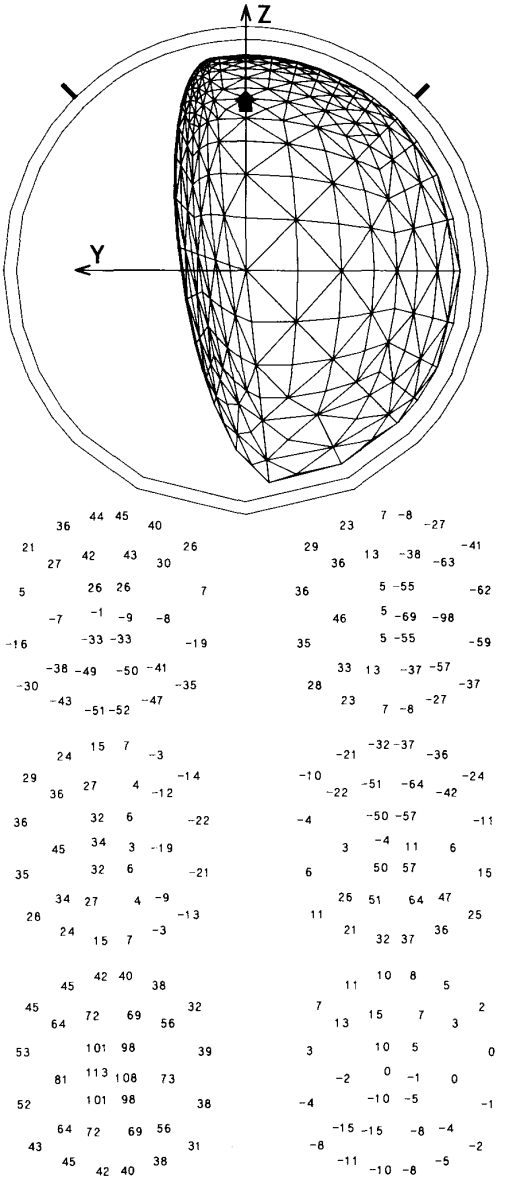

Fig. 8. The "brain-pan" (BP) model. This is similar to the *S* model except that the brain skull surface has been significantly modified. Note that a side view of the model is given here, so that the axes are different than those for the maps. The two marks on the outer surface of the model indicate the extent of the measurement grid.

ments are made. The results for the BP model indicate that even such large deviations may not be a serious cause of localization error. With the exception of the MEG P_z solution, it is primarily the amplitudes and orientations, not the locations, of the solutions for this model which are altered. The errors in the solution amplitudes are as large as approximately 50 percent, but these errors are not a serious concern since, for most purposes, it is accurate localization of a source which is important.

These results also indicate that most general deviations of the head from sphericity do not cause a dipolar source which is perpendicular to the surface of the head to produce significant magnetic fields. It is only for the large deviation of the BP model that the amplitude of the MEG solution for such a source is greater than 6 percent of the actual source amplitude. The location of this source on the "brain pan" surface is consistent with the theory [15] concerning the production of secondary sources at surfaces between regions of different conductivity. Note that such secondary sources are also produced at the spherical

interfaces, but they do not produce a magnetic field component perpendicular to the surface of the sphere which is the component considered in this study and the one used most often in actual measurements.

The localization errors for the EEG solutions are somewhat larger than for the MEG solutions. In addition, some of the EEG solutions have dipole components which are not present in the actual source. Such components are generally associated with EEG solutions which are shifted laterally with respect to the actual source location. However, the differences in the effects of the deviations considered in this study on the EEG and MEG solutions are not significant.

While some deviations do produce maps with significant nondipolar features, most do not. This is indicated by the relatively small (less than approximately 20 percent) F values for most of the solutions. By comparison, a previous study [13] has found that EEG's or MEG's which contain 10 percent noise will produce solutions with F values of approximately 30 percent. Aside from the MEG P_z solutions in all models and the MEG P_x solution in the BP model, the largest F values occur for the MEG P_x and P_y solutions for the NE and WES models. These models have the greatest variations in the radii of curvature of different portions of the measurement grid. The F values of the EEG solutions are generally smaller than those of the MEG solutions because the EEG solution dipole has three components rather than just two as for the MEG solution; increasing the degrees of freedom in a source model increases its ability to fit the surface data.

In summary, these results indicate that the general, nonspherical shape of the head causes localization errors of approximately 1 cm or less for cortical sources when a spherical head model of appropriate size is used for the inverse solution calculations. If this degree of localization accuracy is acceptable, then inverse solutions can be performed on small, inexpensive computers because the necessary calculations are quite simple for such a model. This would make source localization a practical tool for clinical and research use. While these results indicate that general, nonspherical head shape is not likely to be a limitation in the development of such a tool, further research is needed to obtain information about the effect of other volume conductor properties of the head, e.g., holes in the skull and local variations in shape, on localization accuracy.

Appendix

The effects of the different conductivity layers in a multilayer sphere on the EEG moving dipole solutions are taken into account using the following method. First, a moving dipole solution is calculated in a homogeneous sphere, i.e., one with uniform conductivity throughout. Then a second, special moving dipole solution is calculated in a multilayer sphere. In this second solution, the dipole is restricted to be on a fixed radial line which has the same direction as that of the solution in the homogeneous sphere. Therefore, only the amplitudes of the three components of the solution dipole and its depth are free to vary in this special solution. This solution is readily calculated since the partial derivatives with respect to these parameters are easy to calculate from the mathematical expression for potentials produced by a dipole in a multilayer sphere; these derivatives are required in calculating moving dipole solutions [16]. The expression for the potential, in spherical coordinates, is [17]

$$V = \frac{1}{4\pi} \sum_{n=1}^{\infty} f^{n-1} \left[P_r P_n^0(\cos\theta) + \frac{(P_\theta \cos\phi - P_\phi \sin\phi) P_n^1(\cos\theta)}{n} \right] K_n \quad (2)$$

where P_r, P_θ, and P_ϕ are dipole components, f is the radial distance of the dipole, P_n^0 and P_n^1 are associated Legendre polynomials, and K_n is a factor determined by the geometry and conductivities of the multilayer sphere. Inspection of (2) shows that the partial derivatives with respect to P_r, P_θ, P_ϕ, and f are simple to evaluate. This two-step method has been tested and found to work very well, i.e., the solution is located within 0.1 cm of the known source when it is used with calculated data.

References

[1] J. P. Ary, S. A. Klein, and D. H. Fender, "Location of sources of evoked scalp potentials: Corrections for skull and scalp thicknesses," *IEEE Trans. Biomed. Eng.*, vol. BME-28, pp. 447-452, 1981.

[2] J. G. Witwer, G. J. Trezek, and D. L. Jewett, "The effect of media inhomogeneities upon intracranial electric fields," *IEEE Trans. Biomed. Eng.*, vol. BME-19, pp. 352-362, 1972.

[3] C. J. Henderson, S. R. Butler, and A. Glass, "The localization of equivalent dipoles of EEG sources by the application of electric field theory," *Electroencephalogr. clin. Neurophysiol.*, vol. 39, pp. 117-130, 1975.

[4] D. B. Smith, R. D. Sidman, H. Flanigin, J. Henke, and D. Labiner, "A reliable method for localizing deep intracranial sources of the EEG," *Neurol.*, vol. 35, pp. 1702-1707, 1985.

[5] B. He, T. Musha, Y. Okamoto, S. Homma, Y. Nakajima, and T. Sato, "Electric dipole tracing in the brain by means of the boundary element method and its accuracy," *IEEE Trans. Biomed. Eng.*, vol. BME-34, pp. 406-414, 1987.

[6] D. S. Barth, W. Sutherling, J. Broffman, and J. Beatty, "Magnetic localization of a dipolar current source implanted in a sphere and a human cranium," *Electroencephalogr. clin. Neurophysiol.*, vol. 63, pp. 260-273, 1986.

[7] H. Weinberg, P. Brickett, F. Coolsma, and M. Baff, "Magnetic localization of intracranial dipoles: Simulation with a physical model," *Electroencephalogr. clin. Neurophysiol.*, vol. 64, pp. 159-170, 1986.

[8] M. S. Hamalainen and J. Sarvas, "Feasibility of the homogeneous head model in the interpretation of neuromagnetic fields," *Phys. Med. Biol.*, vol. 32, pp. 91-98, 1987.

[9] J. W. H. Meijs, B. J. ten Voorde, M. J. Peters, C. J. Stok, and F. H. Lopes da Silva, "The influence of various head models on EEG's and MEG's," in *Functional Brain Imaging*, G. Pfurtscheller and F. H. Lopes da Silva, Eds. Toronto: Huber, 1988, pp. 31-46.

[10] A. C. L. Barnard, I. M. Duck, M. S. Lynn, and W. P. Timlake, "The application of electromagnetic field theory to electrocardiog-

raphy. II. Numerical solution of the integral equation," *Biophys. J.*, vol. 7, pp. 463-491, 1967.
[11] B. M. Horacek, "Digital models for studies in magnetocardiography," *IEEE Trans. Magn.*, vol. MAG-9, pp. 440-444, 1973.
[12] M. S. Hamalainen and J. Sarvas, "Realistic conductivity geometry model of the human head for interpretation of neuromagnetic data," *IEEE Trans. Biomed. Eng.*, vol. BME-36, pp. 165-171, 1989.
[13] B. N. Cuffin, "A comparison of moving dipole inverse solutions using EEG's and MEG's," *IEEE Trans. Biomed. Eng.*, vol. BME-32, pp. 905-910, 1985.
[14] F. Grynszpan and D. B. Geselowitz, "Model studies of the magnetocardiogram," *Biophys. J.*, vol. 13, pp. 911-925, 1973.
[15] D. B. Geselowitz, "On the magnetic field generated outside an inhomogeneous volume conductor by internal current sources," *IEEE Trans. Magn.*, vol. MAG-6, pp. 346-347, 1970.
[16] D. W. Marquardt, "An algorithm for least-squares estimates of nonlinear parameters," *J. Soc. Ind. Appl. Math.*, vol. 11, pp. 431-441, 1963.
[17] B. N. Cuffin and D. Cohen, "Comparison of the magnetoencephalogram and electroencephalogram," *Electroencephalogr. clin. Neurophysiol.*, vol. 47, pp. 132-146, 1979.

B. Neil Cuffin received the B.S., M.S., and Ph.D. degrees in electrical engineering from The Pennsylvania State University, University Park.

He is currently a Staff Scientist at the Francis Bitter National Magnet Laboratory at Massachusetts Institute of Technology, Cambridge. His research interests are in studies of the information that measurements of the electrical potentials and magnetic fields of the human body can provide about electrical sources in various organs in the body such as the heart and brain.